Two Realms of Brain Dynamics: A Quantum Synaptic Trigger and a Classical Stochastic Neural Field

Moninder Singh Modgil[1] Dnyandeo Dattatray Patil[2]
Cosmos Research Labs
[1]msmodgil@gmail.com [2]cosmoslabsresearch@gmail.com

June 2026

Abstract

We develop a physics of cortical dynamics in which a microscopic quantum realm and a macroscopic classical realm coexist and are coupled at the synapse. Following Beck and Eccles, the trigger for synaptic exocytosis is treated as a genuine quantum event governed by the position–momentum uncertainty relation (Part I); its environmental decoherence is a measurement event in the von Neumann sense [1], and the population of such events seeds the noise of a classical stochastic neural field whose Martin–Siggia–Rose–Janssen–De Dominicis path integral organizes cortical fluctuations through a single parameter $\hbar_{\mathrm{B}} = D = D_{\mathrm{thermal}} + D_{\mathrm{quantum}}$, so that part of the cortical noise descends from $\hbar$ (Part II). Measurement event and perceptual decision are unified as one first-passage construction (Part III). We estimate $\hbar_{\mathrm{B}}$ from cortical parameters, validate the first-passage law numerically, obtain a falsifiable kinetic-isotope and temperature signature in synaptic release, decision error rate, and reaction-time variability, and read the architecture as a quantum–classical hybrid computer. We then derive (Part IV) the cortical fluctuation spectrum from a fluctuation–dissipation relation and compare it to the $1/f$ power of EEG/LFP; develop the stochastic thermodynamics of the neural field, giving the brain's effective Boltzmann scale and the Landauer cost of the synaptic measurement; and map brain states, criticality and neuronal avalanches, and predictive-coding precision onto modulation of $\hbar_{\mathrm{B}}$. The quantum realm is real but confined to the molecular trigger; the classical realm governs cognition; all dualist interpretation is kept outside the physics.

1 Introduction

Cortical activity at the scale of populations is classical and stochastic, yet synaptic transmission — on which all of it rests — is a probabilistic, molecular event. We take the view that the brain is irreducibly a *two-realm* system: a quantum realm at the molecular scale of synaptic release, and a classical stochastic realm at the scale of cortical population activity, coupled at the synapse. The quantum-to-classical transition between them is a measurement, treated rigorously as a spacetime-localized von Neumann measurement [1, 2]. The present paper develops the brain physics: the synaptic quantum trigger (Part I), the classical stochastic neural field it seeds (Part II), the first-passage structure that unifies measurement and decision (Part III), and a set of extensions and predictions — the fluctuation spectrum, the thermodynamics of the field, and brain states — that follow (Part IV). We adopt the Beck–Eccles quantum trigger [5, 6] as a central mechanism while keeping its dualist interpretation strictly outside the physics, and we confine all quantum content

to the decoherence-limited molecular trigger, so that the decoherence objection [4] that defeats theories of sustained neural coherence does not arise.

Part I. The synaptic quantum trigger (the quantum realm)

2 Exocytosis as a quantum two-state trigger

Synaptic transmission is probabilistic: a presynaptic action potential elicits release of a neurotransmitter vesicle with probability $p \sim 0.1$–0.5 per bouton, not with certainty [9]. Following Beck and Eccles [5, 6], we take as a *central mechanism* that the trigger initiating exocytosis is a quantum transition of a light collective coordinate q of the presynaptic release machinery (the paracrystalline vesicular grid), and that this is where a genuine quantum realm resides in the brain.

Model the trigger by a one-dimensional two-state Hamiltonian

$$H_{\mathrm{trig}} = \frac{p_q^2}{2M} + V(q), \tag{1}$$

with effective mass M of order a few atomic mass units and a potential $V(q)$ presenting a barrier of height V_0 and width a separating the closed configuration $|C\rangle$ (no release) from the open configuration $|O\rangle$ (release). The release probability over the trigger interval t_{trig} is the transition probability

$$p = \left|\langle O|\, e^{-iH_{\mathrm{trig}}t_{\mathrm{trig}}/\hbar}\, |C\rangle\right|^2 \;=\; p_{\mathrm{thermal}} + p_{\mathrm{tunnel}}(\hbar), \tag{2}$$

with $p_{\mathrm{tunnel}} \sim \exp\!\big(-\tfrac{2}{\hbar}\int\sqrt{2M(V-E)}\,dq\big)$ in the WKB regime.

2.1 Position–momentum uncertainty enters the trigger

The defining feature, emphasized by Eccles, is that the trigger coordinate cannot be simultaneously localized at $|C\rangle$ with definite (zero) momentum:

$$\Delta q\,\Delta p_q \;\geq\; \frac{\hbar}{2}. \tag{3}$$

The irreducible zero-point spread Δq permits barrier penetration. Quantitatively, the quantum delocalization of q is set by the thermal de Broglie wavelength $\lambda_{\mathrm{dB}} = \hbar/\sqrt{2Mk_BT}$. For $M \approx 6\,u$ and $T = 310\,\mathrm{K}$,

$$\lambda_{\mathrm{dB}} = \frac{\hbar}{\sqrt{2Mk_BT}} \approx 1.1\times10^{-11}\,\mathrm{m} \;\sim\; 10\ \mathrm{pm}, \tag{4}$$

comparable to the picometre barrier widths of the Beck–Eccles trigger. When $\lambda_{\mathrm{dB}} \gtrsim a$, equivalently below the crossover temperature $T_c = \hbar\omega_b/2\pi k_B$ set by the barrier frequency ω_b, tunnelling and zero-point delocalization dominate over classical thermal hopping, and (3) controls the outcome. This is the quantitative sense in which a quantum realm is present: not as sustained coherence, but as the uncertainty-governed rate of a one-shot molecular transition.

3 The trigger as a von Neumann measurement event

The exocytosis trigger is precisely a von Neumann measurement chain, instantiated in biological hardware:

von Neumann chain	**Synaptic trigger**
System in superposition	Trigger coordinate q: $a\|C\rangle + b\|O\rangle$
Internal projection π	$\|O\rangle\langle O\|$ (release outcome)
Overlap / threshold crossing	q crossing the barrier (first passage)
Apparatus / pointer	Vesicle-fusion machinery; quantal release
Recording medium	Postsynaptic potential
Decoherence (the projection)	Synaptic thermal/ionic environment

The trigger interval $t_{\text{trig}} \sim 10^{-13}\,\text{s}$ is shorter than the synaptic decoherence time, so the transition occurs quantum-mechanically; immediately thereafter the environment reduces q to a definite $|C\rangle$ or $|O\rangle$. Decoherence is not an obstacle here but the very mechanism of the quantum-to-classical reduction — it is what makes the synapse a measurement apparatus. The Born probability, $\|\pi\Phi(p)\|^2$, is the release probability p of (2); the threshold crossing of the measurement-event threshold is the barrier crossing of q. The abstract von Neumann observer acquires, at the synapse, a concrete physical realization.

Remark 1 (Interpretation, fenced off)**.** Eccles attached to this mechanism a dualist-interactionist interpretation in which a mental agency biases the release probability p [6]. That interpretation is *not* part of the present physics: it posits no falsifiable dynamics and is excluded from every result here. We retain only the physical claim — that the exocytosis trigger is a quantum transition — and treat p as fixed by (1)–(2).

Part II. The classical stochastic cortical field (the classical realm)

4 The neural field and its path integral

Above the synapse the description is classical and stochastic. Let $\phi(x,t)$ be a coarse-grained cortical activity field over cortical/retinotopic coordinates x, obeying the stochastic Wilson–Cowan / Amari equation [10, 11]

$$\tau_0\,\partial_t\phi(x,t) = -\phi(x,t) + \int dx'\, w(x-x')\, g\big(\phi(x',t)\big) + I(x,t) + \xi(x,t), \tag{5}$$

with synaptic kernel w, sigmoidal gain g, drive I, and Gaussian noise $\langle\xi(x,t)\xi(x',t')\rangle = 2D\,\delta(x-x')\delta(t-t')$. Crucially, ξ is *the population-summed exocytosis noise of Part I*: each released vesicle is a quantum-triggered, classically-recorded event, and the field is their coarse-grained sum.

Enforcing (5) and averaging over the noise introduces a response field $\tilde\phi$ and yields the Martin–Siggia–Rose–Janssen–De Dominicis representation [13, 14]

$$Z = \int \mathcal{D}\phi\,\mathcal{D}\tilde\phi\; e^{S[\phi,\tilde\phi]}, \qquad S = \int dx\,dt\,\Big\{ i\,\tilde\phi\big(\tau_0\partial_t\phi + \phi - \textstyle\int w\,g(\phi) - I\big) - D\,\tilde\phi^2 \Big\}. \tag{6}$$

The factor i is the Fourier representation of the equation-of-motion δ-functional, a calculational device and *not* a quantum phase: the cortical field is classical. This is the second realm, and it does not inherit coherence from the first.

One influence functional, two realms. The path integral (6) and the decoherence of Part I are not separate constructions but two regimes of a single object, the closed-time-path (Schwinger–Keldysh) influence functional [30, 31, 32, 33, 34]. That formalism doubles every degree of freedom onto the forward and backward branches of a closed time contour; its Keldysh decomposition into an *average* field and a *difference* field is precisely the split between the physical field ϕ and the response field $\tilde{\phi}$ used here. The real part of the influence action is a decoherence functional, bilinear in the difference field, that governs the suppression of off-diagonal density-matrix elements — the decoherence which, at the synapse, reduces the trigger of Part I to a definite release outcome. When the difference field plays the role of the MSRJD response field and the system is treated as a classical stochastic process, the same influence functional reduces to the action (6). The quantum-to-classical transition between the realms is thus the decoherence functional itself: Part I is its short-time, off-diagonal-suppressing face, and Part II is its long-time, classical-stochastic face.

5 The fluctuation parameter $\hbar_{\mathrm{B}}$, seeded by the trigger

Rescaling $\tilde{\phi} \to \tilde{\phi}/\sqrt{D}$, the deterministic field equation is the saddle point and fluctuations are organized in powers of D, structurally as $\hbar$ organizes the semiclassical expansion of $\int \mathcal{D}\phi\, e^{iS/\hbar}$. We define the brain's fluctuation parameter

$$\boxed{\hbar_{\mathrm{B}} \equiv D}, \qquad \hbar_{\mathrm{B}} \sim 1/N, \tag{7}$$

N the number of neurons per coarse-graining cell. Unlike a postulated "brain Planck constant" with a fixed joule-second value, $\hbar_{\mathrm{B}}$ is a dimensionless fluctuation strength and a genuine constant of the model.

5.1 Derivation of $\hbar_{\mathrm{B}}$ from synaptic release statistics

This is the quantitative join between the realms. Each synapse releases as a Bernoulli variable of probability p, variance $p(1-p)$. For a coarse-graining cell of N neurons, each receiving K synaptic inputs at rate ν with quantal postsynaptic amplitude q_{syn}, central-limit summation gives the cortical noise amplitude

$$\hbar_{\mathrm{B}} \;=\; D \;\approx\; \frac{K\,\nu\,q_{\mathrm{syn}}^2}{N}\,p(1-p). \tag{8}$$

Observed release probabilities $p \sim 0.1$–0.5 place synapses near the maximum-variance regime of $p(1-p)$, so the cortical realm operates where the seeded noise is large. Substituting the trigger decomposition (2), $p = p_{\mathrm{thermal}} + p_{\mathrm{tunnel}}(\hbar)$,

$$\hbar_{\mathrm{B}} \;=\; D_{\mathrm{thermal}} + D_{\mathrm{quantum}}, \qquad D_{\mathrm{quantum}} \approx \frac{K\nu q_{\mathrm{syn}}^2}{N}\,(1-2p)\,p_{\mathrm{tunnel}}(\hbar). \tag{9}$$

A piece of the classical cortical noise therefore descends from the real $\hbar$ through the quantum trigger. This is the central quantitative content of the two-realms thesis: $\hbar_{\mathrm{B}}$, the organizing parameter of the classical field theory, is *not* free — it is set at the synapse, and carries a quantum imprint.

5.2 Effective temperature, modes, and reframed phenomena

The stationary distribution is $P_{\mathrm{stat}}[\phi] \propto e^{-U[\phi]/D}$ (Freidlin–Wentzell), with an effective noise temperature $T_{\mathrm{eff}} \propto D$ distinct from the thermodynamic 310 K, leaving the real k_B untouched. Linearizing (5) gives coupled normal modes (eigenmodes of the synaptic coupling matrix) mapping

onto neural-mass models [17]; "perceptual collapse" is relaxation to an attractor; waking is drive-clamped, dreaming is unclamped sampling of the quasi-potential; excitatory/inhibitory populations realize "bosonic"/"fermionic" statistics by analogy via the Doi–Peliti and Ising/Hopfield constructions [12, 15, 16]. None of this is quantum: it is the classical realm.

6 Quantitative estimate of $\hbar_{\mathrm{B}}$ and the predicted quantum signature

We now insert realistic cortical numbers into the seeding relation (8)–(9). Define the system-size parameter

$$\Omega := N\,K\,\nu\,\tau_c\,p \tag{10}$$

as the mean number of vesicle-release events per coarse-graining cell per correlation time, with N neurons per cell, K synapses per neuron, mean firing rate ν, correlation time τ_c, and release probability p. The dimensionless fluctuation (loop) parameter is the squared coefficient of variation of the coarse-grained drive,

$$\hbar_{\mathrm{B}} \;=\; \mathrm{CV}^2 \;=\; \frac{1-p}{\Omega} \;=\; \frac{1-p}{N\,K\,\nu\,\tau_c\,p}. \tag{11}$$

Note that the quantal amplitude q_{syn} *cancels* in CV^2, so $\hbar_{\mathrm{B}}$ is independent of that (uncertain) parameter — a useful robustness.

6.1 Magnitude across scales

Taking cortical values $\rho_{\mathrm{neuron}} \approx 5\times10^4\,\mathrm{mm}^{-3}$, $K\approx10^4$, $\nu\approx2\,\mathrm{Hz}$, $\tau_c\approx10\,\mathrm{ms}$, $p\approx0.25$, and the resolution link $\varepsilon=(N/\rho_{\mathrm{neuron}})^{1/3}$:

N (neurons/cell)	ε (mm)	Ω	$\hbar_{\mathrm{B}}=(1-p)/\Omega$	regime
1	0.027	5×10^1	1.5×10^{-2}	single neuron
10	0.058	5×10^2	1.5×10^{-3}	micro-assembly
10^2	0.126	5×10^3	1.5×10^{-4}	minicolumn
10^3	0.271	5×10^4	1.5×10^{-5}	column
10^4	0.585	5×10^5	1.5×10^{-6}	macrocolumn
10^5	1.260	5×10^6	1.5×10^{-7}	cortical area

Thus $\hbar_{\mathrm{B}}\propto1/N$, ranging from $\mathcal{O}(10^{-2})$ at single-neuron resolution to $\mathcal{O}(10^{-6})$ at the macrocolumn scale. Fluctuation corrections to mean-field dynamics are therefore appreciable only for small assemblies; the "interference-relevant" regime $\hbar_{\mathrm{B}}\sim\mathcal{O}(1)$ is approached only near single-quantal-event resolution, $\Omega\sim1$. This is the quantitative meaning of the manuscript-level claim that brain dynamics live near a computable $S/\hbar_{\mathrm{B}}$: it holds at the mesoscale, not the macroscale.

6.2 The quantum imprint and its size

The release probability carries the trigger decomposition $p=p_{\mathrm{thermal}}+p_{\mathrm{tunnel}}(\hbar)$ of (2). From (11), a change δp propagates as

$$\frac{\delta\hbar_{\mathrm{B}}}{\hbar_{\mathrm{B}}} \;=\; -\,\frac{\delta p}{p\,(1-p)}, \qquad p(1-p)=0.19 \text{ at } p=0.25. \tag{12}$$

A quantum (tunnelling) component amounting to $5\%, 10\%, 20\%$ of p shifts the cortical noise amplitude by $+6.7\%, +13\%, +27\%$ respectively — changes well within reach of variance-based synaptic assays, in particular multiple-probability fluctuation analysis (MPFA), which extracts p directly from the variance–mean relation of evoked responses.

6.3 Falsifiable signatures

Two fingerprints distinguish a quantum trigger from a purely thermal one.

(i) Anomalous kinetic isotope effect. In the WKB regime $p_{\text{tunnel}} \propto e^{-B}$ with $B = G\sqrt{M}$ and G mass-independent; primary H/D substitution of the mobile coordinate ($M_D/M_H = 2$) gives $\text{KIE} = p_H/p_D = \exp\big(B_H(\sqrt{2}-1)\big)$:

B_H (tunnelling exponent)	2	3	5	8
$\text{KIE} = p_H/p_D$	2.3	3.5	7.9	27.5

A KIE exceeding the classical semiclassical ceiling (≈ 7) and/or a temperature-independent KIE is the hallmark of tunnelling; it would appear in MPFA-measured p and hence in $\hbar_{\text{B}}$ via (12).

(ii) Sub-Arrhenius temperature dependence. A thermal trigger obeys $p \propto e^{-V_0/k_BT}$; a quantum trigger flattens below the crossover temperature $T_c = \hbar\omega_b/2\pi k_B$ set by the barrier frequency ω_b:

ω_b (s^{-1})	10^{13}	5×10^{13}	10^{14}	2.5×10^{14}
T_c (K)	12	61	122	304

For a stiff, light trigger coordinate ($\omega_b \sim 2.5 \times 10^{14}\,\text{s}^{-1}$) the crossover approaches body temperature — the Beck–Eccles regime — and the thermal de Broglie wavelength $\lambda_{\text{dB}} \approx 11\,\text{pm}$ at $M \approx 6\,u$ (4) is comparable to the barrier width, so tunnelling is non-negligible at 310 K. Observing a deviation from Arrhenius behaviour in release statistics (and in the population Fano factor) as temperature is lowered, with onset near T_c, would be the direct signature; its absence drives $D_{\text{quantum}} \to 0$ and the theory reduces continuously to the purely classical field.

7 Reframed cortical phenomena

The corrected, classical readings of the precursor manuscript's claims are collected for reference: the network path integral is (6); the "cognitive Planck constant" is $\hbar_{\text{B}} = D$ of (7)–(9); the Bose/Fermi neuron classification is a statistics analogy, not quantum exchange symmetry; and inter-brain "entanglement" is replaced by classical correlation/synchrony, since classical channels cannot create entanglement. These corrections confine all quantum content to Part I.

Part III. The bridge: first-passage structure and the two realms

8 Measurement events and perceptual decisions are first-passage times

8.1 The shared structure

The von Neumann measurement event is the first crossing of a threshold by a bounded observable, $\tau_*^{(\eta)} = \inf\{\tau : \Omega_\varepsilon(\tau) \geq \eta\}$. Projecting the cortical field onto a read-out (decision) pattern π,

$$a(t) := \langle \pi, \phi(\cdot, t) \rangle, \qquad \dot{a} = v(a) + \zeta(t), \quad \langle \zeta(t)\zeta(t') \rangle = 2D\,\delta(t - t'), \quad D = \hbar_{\mathrm{B}}, \tag{13}$$

the perceptual decision is the first-passage time $T_*^{(\eta)} = \inf\{t : a(t) \geq \eta\}$. This is the drift–diffusion / bounded-accumulation model of decision [18, 19, 20]. The same first-passage structure thus appears at three levels: the synaptic trigger (barrier crossing of q, Part I), the quantum measurement event (the von Neumann measurement), and the perceptual decision (Part II), bound into one chain:

$$\underbrace{\text{quantum trigger}}_{\text{Part II, } \hbar} \longrightarrow \underbrace{\text{synaptic noise} \Rightarrow \hbar_{\mathrm{B}} = D}_{\text{Eq. (9)}} \longrightarrow \underbrace{\text{perceptual first passage}}_{\text{Part IV}}. \tag{14}$$

8.2 Quantitative link of the resolution scales

The localization scale ε of the von Neumann measurement and the fluctuation strength $\hbar_{\mathrm{B}}$ of the cortical realm are both finite-resolution parameters, linked through the cell population: $N \sim \rho_{\mathrm{neuron}} \varepsilon^n$, so by (7) $\hbar_{\mathrm{B}} = D \sim 1/(\rho_{\mathrm{neuron}} \varepsilon^n)$. Finer localization means fewer neurons per cell and larger fluctuations.

8.3 The two realms, stated precisely

Both realms are real. The brain supports a genuine quantum realm and a genuine classical realm:

- *Quantum realm (Part I):* the synaptic exocytosis trigger — a light collective coordinate whose barrier crossing is governed by $\Delta q\, \Delta p_q \geq \hbar/2$ and tunnelling. It is microscopic ($\sim$pm, $\sim 10^{-13}$s), uncertainty-governed, and decoherence-terminated. The real $\hbar$ acts here.
- *Classical realm (Part II):* the cortical activity field — a classical stochastic field whose path integral (6) carries no physical phase. Cognition, perception, and decision live here, organized by $\hbar_{\mathrm{B}} = D$.

They are coupled, not blurred. The coupling is physical and one-directional in origin: trigger statistics *seed* the cortical noise, $\hbar_{\mathrm{B}} = D_{\mathrm{thermal}} + D_{\mathrm{quantum}}(\hbar)$ (9). The synapse is the locus of the quantum-to-classical transition, described by the von Neumann measurement chain. **Neither realm is reducible to the other.** The classical theory cannot say why D has its value without descending to the quantum trigger; the quantum trigger is cognitively inert until amplified and summed by the classical field. This is the precise sense in which *both quantum and classical descriptions are necessary.*

8.4 A falsifiable signature

The quantum trigger is a central mechanism, and it is falsifiable. Because p_{tunnel} depends on M and $\hbar$ through the WKB action, the model predicts: (i) a *kinetic-isotope effect* — deuteration of the trigger coordinate raises M, shrinks λ_{dB} (4), and reduces p_{tunnel}, shifting release statistics and

hence the cortical noise D beyond the classical mass dependence; (ii) a *low-temperature plateau* — below the crossover T_c, p_{tunnel} becomes temperature-independent, in contrast to the Arrhenius e^{-V_0/k_BT} of a purely thermal trigger. An anomalous isotope or low-temperature dependence of release variance and cortical fluctuation amplitude would be the fingerprint of the quantum realm; its absence would send $D_{\text{quantum}} \to 0$ and reduce the theory continuously to a purely classical field. The framework degrades gracefully, which is a strength.

9 Numerical demonstration: the predicted reaction-time signature

We close with the framework's one concrete, falsifiable computation. We integrate the bounded decision variable (13), $da = v\,dt + \sqrt{2D}\,dW$ with $D = \hbar_{\text{B}}$, by the Euler–Maruyama scheme (step $\Delta t = 5 \times 10^{-4}$, 6×10^4 trials, drift $v = 2$, absorbing bounds at $\pm\eta = \pm 1$ in normalized decision units), recording the first-passage time — the reaction time — and the bound reached — the choice (correct at $+\eta$, error at $-\eta$).

Normalization. The noise strength D used here is that of the *normalized* decision variable $a = \langle \pi, \phi \rangle$, whose absorbing bounds are set to $\pm\eta = \pm 1$ in evidence units; it is related to the microscopic fluctuation parameter $\hbar_{\text{B}}$ of §6 by the read-out gain that maps coarse-grained cortical activity onto the accumulator. The illustrative value $D \approx 0.5$ should therefore *not* be read as the macrocolumn $\hbar_{\text{B}}$ of the §6 scaling (which is several orders of magnitude smaller); it is the effective evidence-noise of the decision variable, of order the small-assembly scale, after that normalization. What is invariant under the read-out gain — and what carries the prediction — is the dimensionless signal-to-noise ratio $v\eta/D$ and, crucially, the *fractional* shift $\delta D/D = \delta\hbar_{\text{B}}/\hbar_{\text{B}}$ of (12): a quantum change in release probability rescales the decision noise by the same fraction regardless of the gain, so the predicted *relative* changes in error rate and reaction-time variance (Table 1) are independent of the normalization and of the absolute value of D.

Validation. The simulated correct-response reaction-time density coincides with the analytic inverse-Gaussian first-passage density, and the simulated two-bound error rate agrees with the analytic value $1/(1+e^{v\eta/D})$ to within Monte-Carlo error (Fig. 1A and Table 1). This confirms that the read-out layer realizes the von Neumann measurement event as a genuine first-passage process.

The quantum perturbation. By (12), $\delta\hbar_{\text{B}}/\hbar_{\text{B}} = -\delta p/[p(1-p)]$, so a tunnelling component worth 10% (resp. 30%) of the release probability p raises $\hbar_{\text{B}}$ by 13% (resp. 30%). Deuteration of the trigger coordinate reduces p_{tunnel} and so raises $\hbar_{\text{B}}$ in the same direction. Table 1 lists the resulting decision statistics.

case	$\hbar_{\text{B}} = D$	error rate (sim)	error rate (analytic)	mean RT	RT CV
baseline	0.50	1.80%	1.80%	0.491	0.658
+13% (10% of p quantum)	0.565	2.56%	2.82%	0.481	0.685
+30% (deuterated)	0.650	4.38%	4.41%	0.464	0.708

Table 1: First-passage decision statistics versus the fluctuation parameter $\hbar_{\text{B}}$. A +13% change in $\hbar_{\text{B}}$ raises the error rate by ∼40% relative; a +30% change roughly doubles it. Mean reaction time is comparatively insensitive.

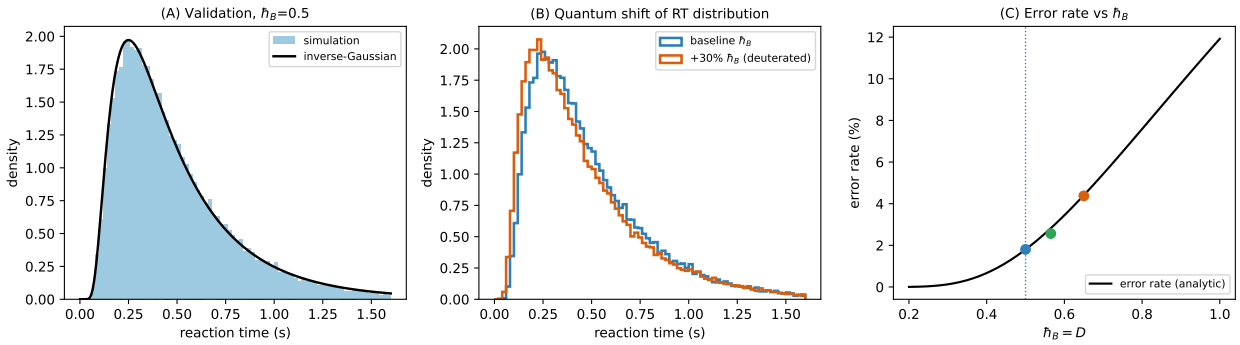

Figure 1: First-passage reaction-time prediction. (A) Simulated correct-response RT density (histogram) against the analytic inverse-Gaussian (line), validating the first-passage construction. (B) The RT distribution broadens and shifts when a quantum perturbation raises $\hbar_{\mathrm{B}}$ (baseline vs. +30%, the deuteration direction). (C) Decision error rate versus $\hbar_{\mathrm{B}}$: simulated points (markers) on the analytic curve $1/(1+e^{v\eta/D})$; the dotted line marks the baseline.

The prediction, stated sharply. Because the inverse-Gaussian mean reaction time η/v is *independent* of D, the signature is carried not by the mean RT but by the *error rate and the RT variability*. A +13% change in $\hbar_{\mathrm{B}}$ — the imprint of a 10% quantum component in p — raises the decision error rate from 1.8% to 2.6% (a ∼40% relative increase) and broadens the RT distribution; a +30% change roughly doubles the error rate. The experimental claim is therefore specific: deuteration of the synaptic trigger coordinate, or cooling below the crossover T_c, should *increase decision error rates and reaction-time variance* by the amount fixed by (12) and (11), while leaving mean reaction time comparatively unchanged. Observation of such a coordinated shift would evidence the quantum realm; its absence drives $D_{\mathrm{quantum}} \to 0$ and the framework reduces continuously to the purely classical neural field.

10 Discussion: the brain as a quantum–classical hybrid and its interface

The two-realm structure of this paper invites a computational reading — the brain as a *hybrid* of a quantum and a classical processor — and lets us state precisely what the interface between the realms is, and how the present framework relates to the Penrose–Hameroff programme.

10.1 The hybrid architecture

A hybrid quantum–classical computer is a quantum subsystem Q and a classical subsystem C joined by two directional channels: a *readout* channel $\mathcal{R}: Q \to C$ (a measurement / POVM collapsing quantum state to classical data) and a *control* channel $\mathcal{K}: C \to Q$ (classical state preparing or biasing the quantum Hamiltonian). The computation is the closed loop

$$Q \xrightarrow{\mathcal{R}} C \xrightarrow{\mathcal{K}} Q. \tag{15}$$

This is exactly the structure of present-day variational / NISQ algorithms [21, 22]: a quantum circuit is measured, a classical optimizer updates parameters, and the circuit is re-prepared. The interface between any quantum and classical computer is precisely this pair $(\mathcal{R}, \mathcal{K})$.

10.2 The readout channel is already present

In this framework $\mathcal{R}$ is the von Neumann measurement chain, realized at the synaptic trigger of Part I: the trigger coordinate's two-state superposition is reduced by the synaptic environment to a definite release / no-release outcome, and the population of such outcomes seeds the classical noise, $\hbar_{\mathrm{B}} = D_{\mathrm{thermal}} + D_{\mathrm{quantum}}$ (9). The quantum-to-classical direction is thus implemented: decoherence *is* the readout.

10.3 The control channel closes the loop

The return channel $\mathcal{K}$ is, in Parts II–III, absent: trigger statistics feed the field but the field does not feed back on the trigger. We close the loop by letting the local classical activity modulate the trigger barrier. Membrane potential and intracellular Ca^{2+} — both monotonic in the local field $\phi(x,t)$ — set the height and width of the exocytosis barrier, so the WKB tunnelling exponent, and hence the tunnelling probability, become functionals of the field,

$$B = B[\phi(x,t)], \qquad p_{\mathrm{tunnel}} = p_{\mathrm{tunnel}}\big[\phi(x,t)\big]. \tag{16}$$

This is the biological counterpart of the microtubule-associated-protein "orchestration" of Orch-OR [23]. Substituting (16) into the seeding relation makes the cortical noise *state-dependent*:

$$\tau_0\,\partial_t\phi = -\phi + \int w\,g(\phi) + I + \xi, \qquad \langle \xi(x,t)\xi(x',t')\rangle = 2\,D[\phi]\,\delta(x-x')\delta(t-t'), \tag{17}$$

with $D[\phi] = D_{\mathrm{thermal}} + D_{\mathrm{quantum}}\big(p_{\mathrm{tunnel}}[\phi]\big)$. The closed loop $\phi \to$ trigger $\to D[\phi] \to \phi$ is the hybrid computation: classical activity sets the quantum trigger statistics, which set the fluctuations driving the classical activity.

10.4 Consequence: multiplicative, activity-dependent noise

Closing the loop converts the additive noise of Part II into *multiplicative* (state-dependent) noise (17) — a concrete, testable dynamical signature. The amplitude of cortical fluctuations should co-vary with local activity through the quantum-imprinted part of $D[\phi]$, and the isotope/temperature dependence of §6 should itself be *modulated by activity level*, strongest where $\partial p_{\mathrm{tunnel}}/\partial\phi$ is largest. Multiplicative noise of this form is known to drive noise-induced transitions and to support self-tuning toward critical regimes, giving the quantum control channel a route to regulate the dynamical state of the classical realm.

10.5 Modest versus ambitious hybrid

Two readings of the hybrid brain share this $(\mathcal{R},\mathcal{K})$ interface but differ in what Q does.

	This framework (modest)	**Orch-OR (ambitious)**
Quantum substrate	synaptic trigger coordinate (light collective mode)	microtubule tubulin qubits
Role of Q	decoherence-limited trigger (a rate)	sustained quantum computation + objective reduction
Coherence required	single event, $\sim 10^{-13}$ s	cognitively relevant, $\sim$ 10–500 ms
Decoherence objection	not an obstacle (no sustained coherence)	central, unresolved [4, 8]
Readout $\mathcal{R}$ ($Q \to C$)	synaptic decoherence = von Neumann chain	objective reduction (OR)
Control $\mathcal{K}$ ($C \to Q$)	$p_{\text{tunnel}}[\phi]$ via membrane/Ca^{2+} (16)	MAPs orchestrate oscillations
Computational claim	classical field computes; Q seeds noise	Q and C both compute
Falsifiable signature	KIE & T-dependence of release/RT (§6, §9)	anaesthetic / isotope effects on consciousness

The modest reading evades the decoherence objection precisely because Q never sustains coherence; the ambitious reading must answer it, and although there is growing evidence of nontrivial quantum phenomena in microtubules — superradiance in tryptophan networks [24], anaesthetic action at quantum-friendly tubulin pockets, nuclear-spin isotope effects — there is as yet no evidence of in-vivo quantum *computation*, and Tegmark's estimate [4] still stands (contested by [8]). The readings are not exclusive: should sustained microtubule coherence be established, Q may be promoted from trigger to processor within the *same* $(\mathcal{R}, \mathcal{K})$ interface. The isotope sensitivity already prominent in this field (xenon nuclear-spin anaesthesia; Fisher's ^{31}P proposal [7]) is the same signature predicted in §6, placing the present hybrid within an existing experimental programme. Quantum-cognition models [25], which use quantum *probability* without a physical quantum substrate, are orthogonal to both readings.

11 How the realms compute together: communication, memory, and division of labour

Section 10 fixed the interface as a readout/control pair $(\mathcal{R}, \mathcal{K})$. We now ask what the two realms actually *do* for each other — how they communicate in both directions, how memory is exchanged, and how the division of computational labour lets the hybrid accomplish what neither realm could alone. The *modest* reading is kept primary (the quantum realm is a memoryless stochastic trigger, not a general processor); we flag where a claim needs the *ambitious* reading.

11.1 The synapse as a codec: two-way communication clocked by spikes

The interface is not continuous but *clocked*: each presynaptic spike opens one trigger event, and between spikes the realms are decoupled. The synapse is therefore a codec (transducer) between a discrete, stochastic, memoryless quantum process and a continuous, persistent classical field.

Readout $\mathcal{R}$ (quantum $\to$ classical) — the write operation. Each trigger decoheres to a binary symbol (release / no-release) drawn with probability p; the classical realm integrates a great many such symbols, across K synapses over a correlation time τ_c, into the continuous field ϕ. The quantum realm writes to the classical realm at an aggregate rate $\sim NK\nu$ symbols per cell per second, each carrying up to $H_2(p) = -p\log_2 p - (1-p)\log_2(1-p)$ bits; this stream is exactly the noise ξ whose amplitude is $\hbar_{\text{B}} = D$. Decoherence *is* the write.

Control $\mathcal{K}$ (classical → quantum) — the load operation. The classical state programs the next trigger: membrane potential and Ca^{2+} (functions of ϕ and of the stored synaptic weights w) set the barrier, $p = p[\phi, w]$ (16). The classical realm thus loads parameters into the quantum subsystem by Hamiltonian preparation — the biological analogue of loading parameters into a variational quantum circuit. Read and load alternate on the spike clock, closing the loop of §10.

11.2 Division of computational labour

The realms cooperate because their physical characters are opposite.

	Quantum trigger realm	**Classical field realm**
Randomness	irreducible (true)	pseudo / deterministic on average
Memory	none — decoheres in $\sim 10^{-13}$ s (Markovian)	persistent (attractors, weights w)
Operation	single-shot, sensitive, amplifying	integrative, averaging, error-correcting
Grain / speed	discrete events, fast	continuous, smoothed, slow
Excels at	generating entropy, breaking ties, exploration	storage, sequence/logic, stable inference
Fails by	no persistence, no context	trapping in local minima, no fresh entropy

11.3 Memory exchange is asymmetric

Persistent memory lives in the classical realm; the quantum trigger is memoryless. The exchange is therefore one of *programming* and *consolidation*, not symmetric storage:

- **Classical → quantum (load).** Stored weights and the current attractor set $p[\phi, w]$, so classical memory programs which trigger transitions are favoured: the classical realm supplies the context the quantum realm cannot itself retain.
- **Quantum → classical (consolidate).** Single-shot release outcomes, accumulated by first passage and fed to synaptic plasticity ($w \to w + \Delta w$ driven by release statistics), are written into durable classical memory. Quantum outputs become classical memories.

In the modest reading there is *no* long-term quantum memory; the ambitious (Orch-OR) reading would permit short-lived microtubule quantum memory, but this is contested and not required here.

11.4 How they help each other accomplish tasks

The cooperation is that of a stochastic sampler with a deterministic integrator — the structure of a variational hybrid algorithm [21, 22] and of noise-exploiting computation in the nervous system [27, 28, 29].

(a) Adaptive annealing (exploration ↔ exploitation). The classical realm poses the problem as a quasi-potential landscape $U[\phi]$ (the stationary weight $P_{\text{stat}} \propto e^{-U[\phi]/D}$ of §5); the quantum realm supplies the exploration noise $D = \hbar_{\text{B}}$ that lets the field escape local minima, just as temperature does in simulated annealing [26]. Because control makes $D = D[\phi]$ activity-dependent (§10), the hybrid can *self-anneal*: raise the quantum-sourced noise to explore when the classical state is far from a solution, lower it to commit as it converges. The quantum realm is, in effect, the brain's annealing schedule.

(b) Tie-breaking at balanced evidence. When classical evidence is symmetric (drift $v \to 0$ in (13)), a deterministic accumulator cannot decide — the Buridan problem. The quantum-sourced noise guarantees the first passage (13) still terminates, selecting an outcome in finite time. The quantum realm resolves an indeterminacy the classical realm cannot.

(c) Retrieval, recombination, dreaming. Memory retrieval is noise-assisted descent into the attractor encoding a stored pattern; creative recombination and the unclamped dreaming dynamics of Part II are the high-D regime in which quantum-seeded fluctuations sample broadly across the quasi-potential. The quantum realm supplies the variability; the classical realm supplies the stored structure being recombined.

(d) Learning. Because plasticity is driven by release statistics, the quantum-imprinted exploration noise feeds directly into weight updates, implementing reinforcement-style exploration: the quantum realm proposes variation, the classical realm selects and consolidates what succeeds.

In every case the labour splits the same way — the quantum realm generates entropy, sensitivity, and exploration; the classical realm supplies memory, integration, and selection. Neither computes the task alone: the classical realm without fresh entropy stalls in local minima and cannot break ties, while the quantum realm without the classical realm has neither memory, context, nor any way to accumulate its single-shot outputs into a result.

11.5 Scope

The phrase "quantum computing system" is fully warranted only in the ambitious reading, where Q performs coherent computation. In the modest reading defended here, Q is a true-random, sensitive, memoryless *sampler and tie-breaker* — computationally valuable, but not a general-purpose quantum processor. The cooperative roles above hold in both readings; only their power differs. The falsifiable signatures remain those of §6–§9.

Part IV. Extensions: spectra, thermodynamics, and brain states

12 The cortical fluctuation spectrum from fluctuation–dissipation

Linearizing the neural field (5) about a stationary state and writing $\delta\phi$ for the deviation, each spatial mode k obeys an Ornstein–Uhlenbeck equation $\tau_0 \partial_t \delta\phi_k = -a(k)\,\delta\phi_k + \xi_k$, with relaxation coefficient $a(k) = 1 - \tilde{w}(k)\,g'$ fixed by the synaptic kernel and gain. The linear response and the fluctuation spectrum are

$$\chi_k(\omega) = \frac{1}{-i\omega\tau_0 + a(k)}, \qquad S_\phi(\omega, k) = 2D\,|\chi_k(\omega)|^2 = \frac{2D}{\omega^2\tau_0^2 + a(k)^2}, \tag{18}$$

a Lorentzian of corner frequency $f_c(k) = a(k)/2\pi\tau_0$ and total power $\propto D = \hbar_{\mathrm{B}}$. Equation (18) is a fluctuation–dissipation relation, $S_\phi = 2D\,|\chi_k|^2$, with $D = \hbar_{\mathrm{B}}$ in the role of $k_B T_{\mathrm{eff}}$. Summed over the cortical mode spectrum — whose corner frequencies are broadly distributed because the coupling $\tilde{w}(k)$ is heterogeneous across scales — the superposed Lorentzians produce an $S(f) \propto 1/f^\beta$ band, the form measured in LFP and EEG [35, 36]. Two quantitative predictions follow: the total spectral power scales linearly with $\hbar_{\mathrm{B}}$, so the kinetic-isotope/temperature perturbation of §6 rescales resting-state spectral power by the fractional shift $\delta\hbar_{\mathrm{B}}/\hbar_{\mathrm{B}}$ of (12); and the spectral exponent β reflects the eigenmode distribution of the synaptic coupling, giving a direct handle on $\tilde{w}(k)$ from the measured spectrum.

13 Stochastic thermodynamics of the neural field

The cortical field is a driven, dissipative non-equilibrium steady state, so stochastic thermodynamics [37] applies. The noise $D = \hbar_{\mathrm{B}}$ enters an Einstein relation $D = \mu\, k_B T_{\mathrm{eff}}$ with mobility μ, which fixes the meaning of a "brain Boltzmann scale": it is not a new fundamental constant but the effective temperature $T_{\mathrm{eff}} = D/(\mu k_B)$ of the seeded noise, distinct from the thermodynamic 310 K. The steady state carries a non-negative entropy-production rate, and transitions between attractors obey the Crooks and Jarzynski fluctuation theorems [38, 39].

The interface of §10 has a thermodynamic cost. Each synaptic readout records one bit (release / no-release) and so, by Landauer's principle [40, 41], dissipates at least $k_B T \ln 2 \approx 3 \times 10^{-21}$ J at $T = 310$ K. The metabolic energy per vesicle cycle is $\sim 10^{-20}$–10^{-19} J, so the synapse operates within one to two orders of the Landauer bound: the brain is a near-thermodynamically-optimal measuring device. Across $\sim 10^{15}$ synapses firing at a few Hz, this readout dissipation is of order the brain's ~ 25 W budget, tying the measurement interface to the organ's energetics.

14 Brain states, criticality, and predictive coding

A single axis — the effective noise $\hbar_{\mathrm{B}} = D$, made activity-dependent by the control channel (16)–(17) — organizes a range of phenomena.

Brain states. Waking is the low-D, drive-clamped regime; dreaming is the high-D, unclamped sampling of the quasi-potential; general anaesthesia suppresses the control channel and the quantum contribution D_{quantum}, collapsing the exploration that sustains wakefulness; psychedelics correspond to elevated D and proximity to criticality, the "entropic brain" [42]. Anaesthesia is the cleanest test, since it also acts on the Beck–Eccles trigger.

Criticality. Organized as a loop expansion in $\hbar_{\mathrm{B}}$, the field near a continuous transition between quiescent and active states has scale-free fluctuations — neuronal avalanches with power-law size and duration distributions [43, 44]. The activity-dependent control channel (17) furnishes a feedback that can self-tune the field toward this critical point, and the framework predicts that the avalanche exponents shift under the same isotope/temperature perturbations that change $\hbar_{\mathrm{B}}$.

Predictive coding. In active-inference terms [45], an attractor is a prior, the first-passage read-out is the inference of a decision, and the control channel $p_{\mathrm{tunnel}}[\phi]$ — by setting the exploration noise $D[\phi]$ — realizes the *precision* (inverse uncertainty) that predictive coding modulates. The quantum realm is then the physical substrate of precision control, supplying the tunable stochasticity that active inference treats as a free parameter.

15 Further directions

Three further consequences follow without additional assumptions. *Stochastic resonance:* signal detection is optimized at a nonzero $\hbar_{\mathrm{B}}$, so deuteration or anaesthesia, by shifting $\hbar_{\mathrm{B}}$, should move detection performance off its peak. *Quantum Darwinism:* a single trigger outcome is redundantly imprinted across the many synapses that integrate it — the broadcast mechanism by which a quantum outcome becomes an objective classical record [3]. *Cerebellar timing:* the timing jitter of a Purkinje read-out is the variance of a first-passage time whose floor is set by $\hbar_{\mathrm{B}}$, giving cerebellar temporal precision a noise-limited bound.

16 Conclusion

We have set out a two-realm physics of the brain. A quantum realm — the Beck–Eccles synaptic exocytosis trigger, governed by position–momentum uncertainty (Part I) — is coupled, through environmental decoherence acting as a von Neumann measurement event, to a classical stochastic neural field whose MSRJD path integral is organized by a single fluctuation parameter $\hbar_{\mathrm{B}} = D = D_{\mathrm{thermal}} + D_{\mathrm{quantum}}$, seeded at the synapse so that part of the cortical noise descends from $\hbar$ (Part II). Measurement and perceptual decision are the same first-passage construction (Part III), from which a numerically validated, falsifiable isotope/temperature signature follows. The extensions of Part IV — the $1/f$ fluctuation spectrum from fluctuation–dissipation, the stochastic thermodynamics and Landauer cost of the synaptic measurement, and the organization of brain states, criticality, and predictive-coding precision along the single axis $\hbar_{\mathrm{B}}$ — show that the framework reaches well beyond its starting point. The quantum realm is real but confined to the molecular trigger; the classical realm governs cognition; the two are coupled, not blurred, at the synapse; and all dualist interpretation is kept outside the physics.

References

[1] J. von Neumann, *Mathematical Foundations of Quantum Mechanics* (Princeton Univ. Press, 1955).

[2] M. S. Modgil, "Axioms for a Differential Geometric approach to von Neumann's Theory of Quantum Measurement," Quantum Speculations **5**, 1 (2023).

[3] W. H. Zurek, "Decoherence, einselection, and the quantum origins of the classical," Rev. Mod. Phys. **75**, 715 (2003).

[4] M. Tegmark, "Importance of quantum decoherence in brain processes," Phys. Rev. E **61**, 4194 (2000).

[5] F. Beck and J. C. Eccles, "Quantum aspects of brain activity and the role of consciousness," Proc. Natl. Acad. Sci. **89**, 11357 (1992).

[6] J. C. Eccles, *How the Self Controls Its Brain* (Springer, 1994).

[7] M. P. A. Fisher, "Quantum cognition: The possibility of processing with nuclear spins in the brain," Ann. Phys. **362**, 593 (2015).

[8] S. Hagan, S. Hameroff, J. A. Tuszyński, "Quantum computation in brain microtubules," Phys. Rev. E **65**, 061901 (2002).

[9] B. Katz, *The Release of Neural Transmitter Substances* (Liverpool Univ. Press, 1969); J. del Castillo and B. Katz, J. Physiol. **124**, 560 (1954).

[10] H. R. Wilson and J. D. Cowan, "Excitatory and inhibitory interactions in localized populations of model neurons," Biophys. J. **12**, 1 (1972).

[11] S. Amari, "Dynamics of pattern formation in lateral-inhibition type neural fields," Biol. Cybern. **27**, 77 (1977).

[12] M. A. Buice and J. D. Cowan, "Field-theoretic approach to fluctuations in neural networks," Phys. Rev. E **75**, 051919 (2007); C. C. Chow and M. A. Buice, "Path integral methods for stochastic differential equations," J. Math. Neurosci. **5**, 8 (2015).

[13] P. C. Martin, E. D. Siggia, H. A. Rose, "Statistical dynamics of classical systems," Phys. Rev. A **8**, 423 (1973).

[14] U. C. Täuber, *Critical Dynamics* (Cambridge Univ. Press, 2014).

[15] J. J. Hopfield, "Neural networks and physical systems with emergent collective computational abilities," Proc. Natl. Acad. Sci. **79**, 2554 (1982).

[16] D. J. Amit, H. Gutfreund, H. Sompolinsky, "Spin-glass models of neural networks," Phys. Rev. A **32**, 1007 (1985).

[17] B. H. Jansen and V. G. Rit, "Electroencephalogram and visual evoked potential generation in a mathematical model of coupled cortical columns," Biol. Cybern. **73**, 357 (1995).

[18] R. Ratcliff, "A theory of memory retrieval," Psychol. Rev. **85**, 59 (1978).

[19] J. I. Gold and M. N. Shadlen, "The neural basis of decision making," Annu. Rev. Neurosci. **30**, 535 (2007).

[20] R. Bogacz et al., "The physics of optimal decision making," Psychol. Rev. **113**, 700 (2006).

[21] J. Preskill, "Quantum computing in the NISQ era and beyond," Quantum **2**, 79 (2018).

[22] M. Cerezo et al., "Variational quantum algorithms," Nat. Rev. Phys. **3**, 625 (2021).

[23] S. Hameroff and R. Penrose, "Consciousness in the universe: A review of the 'Orch OR' theory," Phys. Life Rev. **11**, 39 (2014).

[24] N. S. Babcock et al., "Ultraviolet superradiance from mega-networks of tryptophan in biological architectures," J. Phys. Chem. B **128**, 4035 (2024).

[25] J. R. Busemeyer and P. D. Bruza, *Quantum Models of Cognition and Decision* (Cambridge Univ. Press, 2012).

[26] S. Kirkpatrick, C. D. Gelatt, M. P. Vecchi, "Optimization by simulated annealing," Science **220**, 671 (1983).

[27] A. A. Faisal, L. P. J. Selen, D. M. Wolpert, "Noise in the nervous system," Nat. Rev. Neurosci. **9**, 292 (2008).

[28] G. Deco, E. T. Rolls, "Stochastic dynamics as a principle of brain function," Prog. Neurobiol. **88**, 1 (2009).

[29] M. D. McDonnell, L. M. Ward, "The benefits of noise in neural systems," Nat. Rev. Neurosci. **12**, 415 (2011).

[30] R. P. Feynman and F. L. Vernon, "The theory of a general quantum system interacting with a linear dissipative system," Ann. Phys. **24**, 118 (1963).

[31] J. Schwinger, "Brownian motion of a quantum oscillator," J. Math. Phys. **2**, 407 (1961).

[32] L. V. Keldysh, "Diagram technique for nonequilibrium processes," Sov. Phys. JETP **20**, 1018 (1965).

[33] E. A. Calzetta and B. L. Hu, *Nonequilibrium Quantum Field Theory* (Cambridge Univ. Press, 2008).

[34] A. Kamenev, *Field Theory of Non-Equilibrium Systems* (Cambridge Univ. Press, 2011).

[35] B. J. He, "Scale-free brain activity: history, time scales, dynamics," Trends Cogn. Sci. **18**, 480 (2014).

[36] A. Bédard and A. Destexhe, "Macroscopic models of local field potentials and a model of $1/f$ noise," Biophys. J. **96**, 2589 (2009).

[37] U. Seifert, "Stochastic thermodynamics, fluctuation theorems and molecular machines," Rep. Prog. Phys. **75**, 126001 (2012).

[38] G. E. Crooks, "Entropy production fluctuation theorem and the nonequilibrium work relation," Phys. Rev. E **60**, 2721 (1999).

[39] C. Jarzynski, "Nonequilibrium equality for free energy differences," Phys. Rev. Lett. **78**, 2690 (1997).

[40] R. Landauer, "Irreversibility and heat generation in the computing process," IBM J. Res. Dev. **5**, 183 (1961).

[41] J. M. R. Parrondo, J. M. Horowitz, T. Sagawa, "Thermodynamics of information," Nat. Phys. **11**, 131 (2015).

[42] R. L. Carhart-Harris et al., "The entropic brain," Front. Hum. Neurosci. **8**, 20 (2014).

[43] J. M. Beggs and D. Plenz, "Neuronal avalanches in neocortical circuits," J. Neurosci. **23**, 11167 (2003).

[44] D. R. Chialvo, "Emergent complex neural dynamics," Nat. Phys. **6**, 744 (2010).

[45] K. Friston, "The free-energy principle: a unified brain theory?" Nat. Rev. Neurosci. **11**, 127 (2010).